Supporting Information

Density of 1-Butyl-3-methylimidazolium Bis(trifluoromethanesulfonyl)amide and 1-Hexyl-3-methylimidazolium Bis(trifluoromethanesulfonyl)amide over an Extended Pressure Range up to 250 MPa

Mitsuhiro Kanakubo,[*,†] *and Kenneth R. Harris,* [* †,‡]

[†] National Institute of Industrial Science and Technology (AIST), 4-2-1 Nigatake, Miyagino-ku, Sendai 983-8551, Japan

[‡] School of Physical, Environmental and Mathematical Sciences, University of New South Wales, P.O. Box 7916, Canberra BC, ACT 2610, Australia

AUTHOR INFORMATION

Corresponding Authors

*E-mail: m-kanakubo@aist.go.jp, Fax: +81-22-232-7002; k.harris@adfa.edu.au.

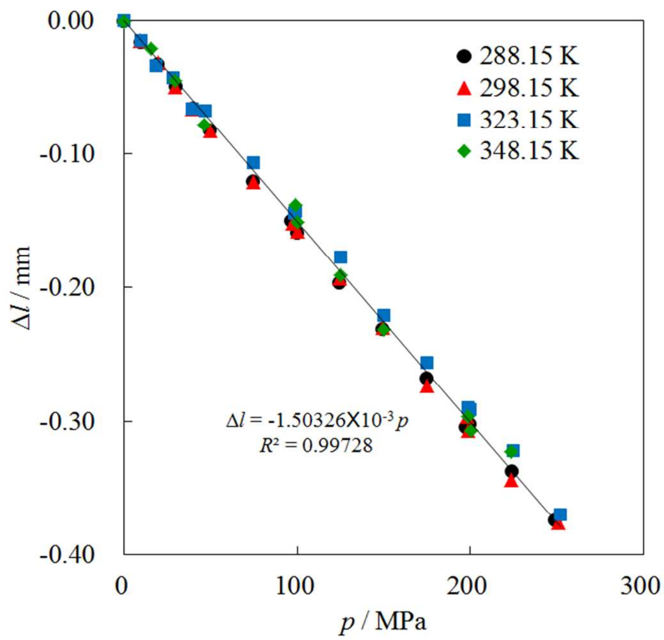

Figure S1. Displacement corrections for the bellows used in this study at high pressures. The following equations were derived for the displacement corrections at different temperatures with the standard uncertainty for the slopes; (Δl/mm) = -1.503(±0.008)×10^{-3} (p/MPa) at 288.15 K, (Δl/mm) = -1.533(±0.009)×10^{-3} (p/MPa) at 298.15 K, (Δl/mm) = -1.455(±0.008)×10^{-3} (p/MPa) at 323.15 K, and (Δl/mm) = -1.492(±0.014)×10^{-3} (p/MPa) at 348.15 K. They were regarded as independent of temperature: (Δl/mm) = -1.50326(±0.00615)×10^{-3} (p/MPa).

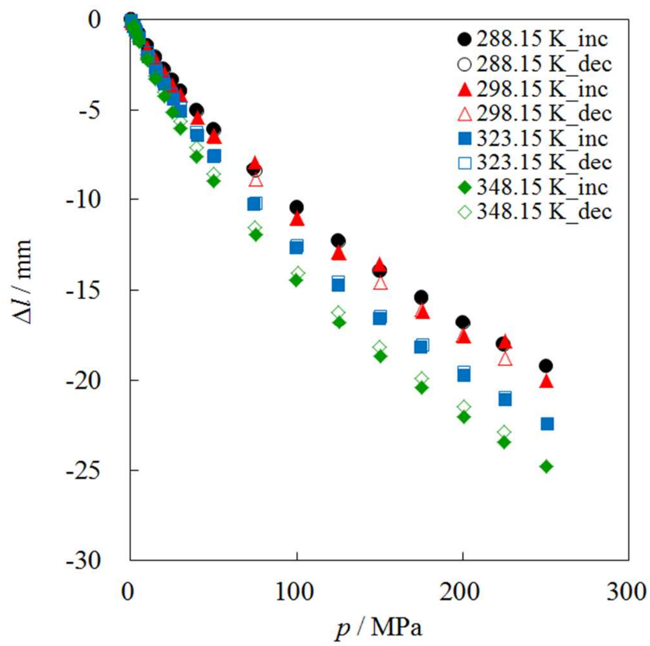

Figure S2. Pressure dependence of the displacement Δ*l* for toluene at different temperatures. The initial positions l_0 were determined with 8th order polynomial fits at each temperature when *p* was both increased and decreased.

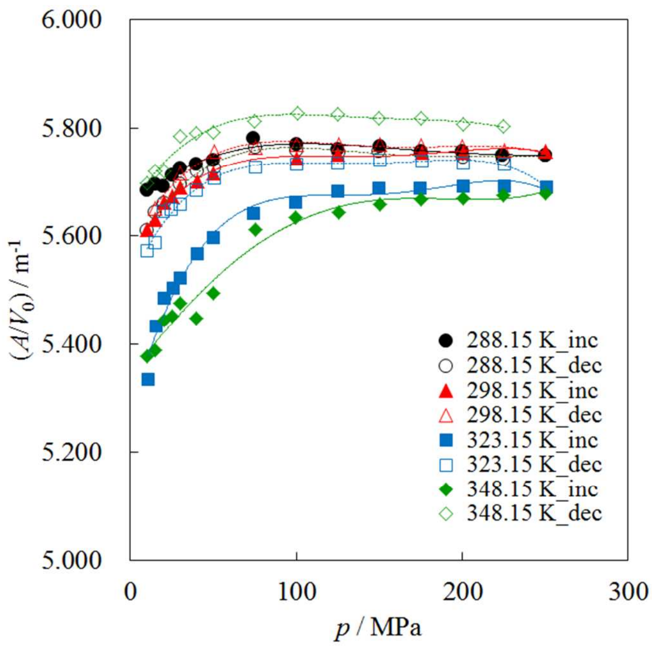

Figure S3. Plots of (A/V_0) against p for toluene at different temperatures. The results show a slight temperature dependence and pressure hysteresis: therefore, the data were fitted to separate 4th order polynomial equations at each temperature when p was both increased and decreased. The regressed equations are summarized in **Table S1**.

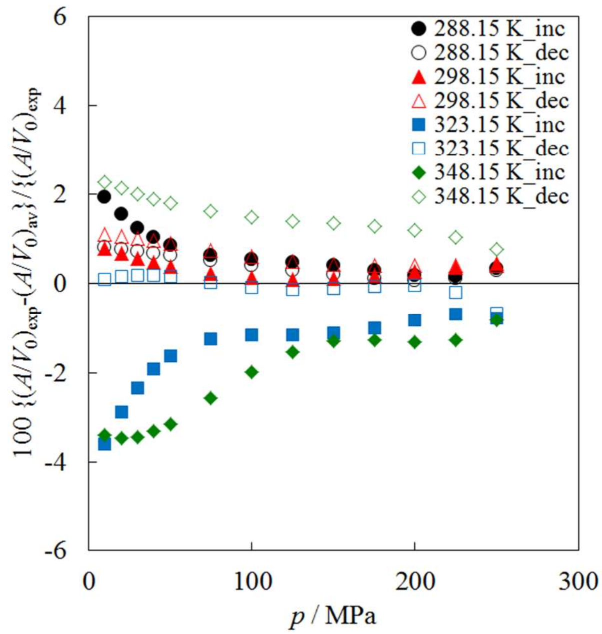

Figure S4. Pressure dependence of the difference of (A/V_0) from the average at different temperatures. The average was obtained at each pressure.

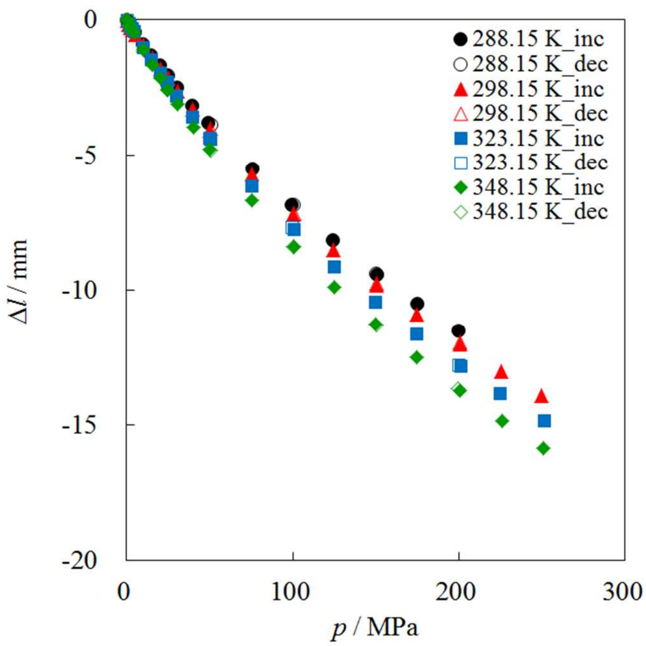

Figure S5. Pressure dependence of the displacement Δl for [BMIM][Tf_2N] at different temperatures. The initial positions l_0 were determined from 8th order polynomial fits at each temperature when p was increased and decreased, respectively.

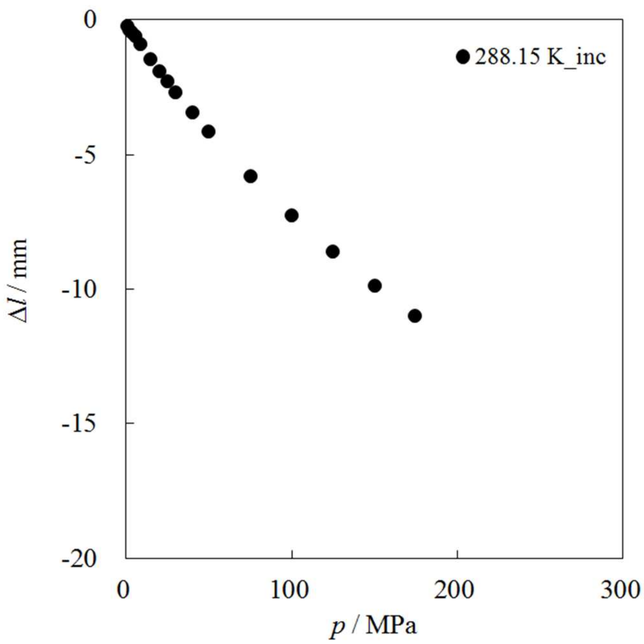

Figure S6. Pressure dependence of the displacement Δl for [HMIM][Tf_2N] at 288.15 K. The initial positions l_0 were determined from an 8th order polynomial fit.

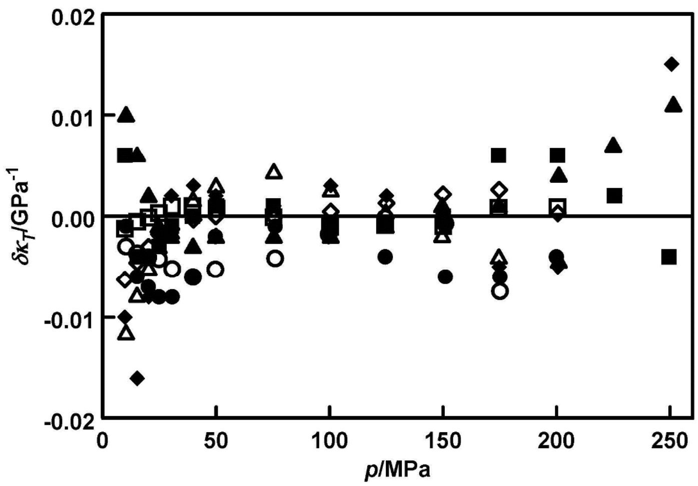

Figure S7. Deviations of isothermal compressibilities for [BMIM][TF$_2$N] (κ_T) calculated by the spline fitting method (closed symbols) and from the secant bulk modulus (open symbols) from those calculated from differentiation of the Tait equation of state. Circles, 283.2K; squares, 298.2 K; triangles, 323.2 K; diamonds, 348.2 K. As mentioned in the text, the spline method results in slightly more scatter.

Table S1. Values of coefficients for the 4th order polynomial equation, $(A/V_0) = e_0 + e_1p + e_2p^2 + e_3p^3 + e_4p^4$, for toluene as given in **Figure S3**.

T / K	p change	e_0/m^{-1}	e_1/10^{-3} m^{-1}·MPa^{-1}	e_2/10^{-5} m^{-1}·MPa^{-2}	e_3/10^{-7} m^{-1}·MPa^{-3}	e_4 /10^{-10} m^{-1}·MPa^{-4}	σ/%
288.15	increasing	5.6527	2.9483	-2.5080	0.84048	-0.98756	0.09
	decreasing	5.5672	5.5846	-5.5442	2.2490	-3.2400	0.38
298.15	increasing	5.5686	5.2435	-5.5648	2.5164	-4.0400	0.12
	decreasing	5.5807	5.8815	-6.2937	2.7953	-4.4349	0.13
323.15	increasing	5.2684	11.376	-11.697	5.1909	-8.2628	0.36
	decreasing	5.5171	6.7679	-7.6378	3.6936	-6.4382	0.17
348.15	increasing	5.3433	4.0736	-0.93860	-0.48239	1.6917	0.39
	decreasing	5.6520	5.1614	-5.5256	2.5126	-4.2021	0.20

Table S2. Values of κ_T, α_p and p_{int} for [BMIM][Tf_2N] as a function of T and p obtained with different methods.

T/K	p/MPa	κ_T/GPa^{-1}	κ_T/GPa^{-1}	$10^3\alpha_p$/K^{-1}	p_{int}
experimental (T,p)		Tait	Spline fitting	Tait	Tait
288.15	10.32	0.486	0.485	0.650	375
288.15	15.13	0.474	0.468	0.643	376
288.15	20.09	0.462	0.455	0.637	377
288.15	24.82	0.451	0.443	0.631	378
288.15	30.62	0.439	0.431	0.624	379
288.15	39.77	0.421	0.415	0.613	380
288.15	49.64	0.402	0.400	0.603	382
288.15	76.0	0.361	0.360	0.578	385
288.16	99.6	0.331	0.329	0.559	387
288.15	124.5	0.305	0.301	0.542	387
288.15	151.0	0.281	0.275	0.525	387
288.15	175.1	0.263	0.257	0.512	387
288.15	199.9	0.246	0.242	0.500	385
298.15	9.76	0.502	0.508	0.651	376
298.15	15.20	0.488	0.484	0.643	378
298.16	20.12	0.476	0.472	0.636	379
298.15	24.77	0.465	0.462	0.630	380
298.16	30.40	0.452	0.451	0.623	381
298.15	39.56	0.433	0.433	0.612	382
298.16	50.11	0.413	0.414	0.601	384
298.16	75.2	0.372	0.373	0.577	387
298.16	100.2	0.339	0.338	0.556	389
298.15	124.5	0.312	0.311	0.539	390
298.16	150.1	0.289	0.289	0.523	390
298.15	174.4	0.269	0.275	0.509	389
298.15	200.4	0.252	0.258	0.496	387

298.16	225.5	0.237	0.239	0.484	384
298.15	249.6	0.224	0.220	0.474	381
323.16	10.25	0.540	0.530	0.650	379
323.15	15.15	0.525	0.519	0.642	380
323.16	20.18	0.511	0.509	0.635	381
323.15	24.67	0.499	0.500	0.628	382
323.15	30.10	0.486	0.488	0.621	383
323.15	39.78	0.463	0.466	0.608	385
323.15	49.91	0.442	0.444	0.597	386
323.15	75.4	0.396	0.398	0.570	390
323.15	100.5	0.360	0.362	0.549	392
323.15	124.7	0.331	0.332	0.530	393
323.15	149.6	0.306	0.305	0.514	393
323.15	174.6	0.285	0.284	0.499	392
323.16	201.0	0.265	0.261	0.485	390
323.15	225.0	0.250	0.243	0.474	387
323.15	251.5	0.235	0.224	0.462	384
348.15	9.76	0.584	0.574	0.650	377
348.15	15.20	0.566	0.550	0.640	379
348.15	20.22	0.550	0.542	0.632	380
348.15	24.83	0.536	0.534	0.625	381
348.15	30.30	0.521	0.523	0.617	382
348.15	39.98	0.496	0.499	0.604	384
348.15	49.89	0.473	0.475	0.591	385
348.15	75.4	0.423	0.424	0.563	389
348.15	100.5	0.383	0.386	0.540	390
348.15	125.1	0.351	0.353	0.521	391
348.15	150.0	0.324	0.323	0.503	391
348.15	174.7	0.301	0.296	0.488	389
348.15	200.6	0.281	0.276	0.474	387
348.15	225.7	0.263	0.265	0.461	384

348.15	250.7	0.248	0.263	0.450	380

Secant bulk modulus method.

T/K	p/MPa	K/MPa	V_m/cm^{3}mol^{-1}	κ_T/GPa^{-1}	$10^3\alpha_p$/K^{-1}	p_{int}/MPa
288.15	0.1		289.97	0.512	0.6656	374
288.15	10	1986.9	288.51	0.484	0.661	383
288.15	25	2090.1	286.51	0.446	0.644	390
288.15	50	2246.7	283.52	0.396	0.604	390
288.15	75	2388.0	280.87	0.358	0.567	381
288.15	100	2518.4	278.46	0.329	0.538	372
288.15	125	2642.6	276.26	0.304	0.518	365
288.15	150	2765.0	274.24	0.281	0.503	365
288.15	175	2890.2	272.42	0.256	0.486	372
288.15	200	3022.6	270.79	0.224	0.459	390
298.15	0.1		291.91	0.526	0.6660	378
298.15	10	1882.8	290.36	0.500	0.658	382
298.15	25	1988.3	288.24	0.465	0.640	385
298.15	50	2149.7	285.12	0.414	0.602	384
298.15	75	2295.6	282.37	0.372	0.567	379
298.15	100	2428.9	279.89	0.338	0.540	376
298.15	125	2552.4	277.61	0.311	0.519	373
298.15	150	2669.1	275.50	0.288	0.503	370
298.15	175	2781.9	273.55	0.269	0.486	362
298.15	200	2893.7	271.73	0.253	0.462	344
323.15	0.1		296.8	0.553	0.6668	390
323.15	10	1852.3	295.21	0.529	0.651	388

323.15	25	1921.9	292.95	0.495	0.629	385
323.15	50	2039.2	289.54	0.445	0.596	384
323.15	75	2157.5	286.50	0.401	0.567	379
323.15	100	2276.4	283.78	0.363	0.543	376
323.15	125	2395.4	281.33	0.331	0.521	373
323.15	150	2513.9	279.10	0.304	0.502	370
323.15	175	2631.4	277.07	0.281	0.484	362
323.15	200	2747.3	275.21	0.261	0.467	344
348.15	0.1		301.81	0.608	0.6674	390
348.15	10	1671.6	300.00	0.577	0.644	388
348.15	25	1754.6	297.51	0.534	0.619	385
348.15	50	1886.3	293.81	0.473	0.590	383
348.15	75	2010.7	290.55	0.424	0.568	382
348.15	100	2129.2	287.63	0.384	0.546	383
348.15	125	2243.0	284.99	0.352	0.523	384
348.15	150	2353.6	282.57	0.326	0.501	384
348.15	175	2462.1	280.35	0.303	0.483	382
348.15	200	2570.0	278.32	0.282	0.473	378